RESEARCH ARTICLE

A new methodology to characterize the kinetics of a seed during the imbibition process

D. Moret-Fernández · J. Tormo · B. Latorre

Abstract

Aims Assuming the saturated, θ_s, and residual θ_r volumetric water contents of a seed as known inputs, we present a methodology to determine the hydraulic properties of a seed: α, n parameters and hydraulic conductivity K_s.

Methods The seed is considered as a porous material in which water flow is governed with the same hydraulic properties defined for soils. Using the HYDRUS-2D software, the hydraulic properties of a seed were estimated from the inverse analysis of several cumulative seed imbibition curves measured at different seed water potentials, h. The optimum number of h was evaluated on synthetic seeds. The theoretical analysis was validated in laboratory experiments on barley, wheat and vetch seeds, where imbibition curves were measured with germination tests at seven levels of h (from 0 to -2.50 MPa).

Results The theoretical analysis showed that accurate estimates of α, n and K_s can be obtained if the most negative h-values are included in the optimization. The sensitivity analysis showed that the method allows obtaining a unique solution of α, n and K_s. The optimization error on the theoretical α, n and K_s was less than 1%. A satisfactory validation was also obtained on the experimental seed imbibition curves, with robust fits between the measured and optimized data. A unique solution of α, n and K_s was also obtained in all cases.

Conclusions A new method to determine the hydraulic properties of a seed is presented. This methodology could be used in different areas involving seed imbibition and also to simulate seed imbibition in different scenarios.

Responsible Editor: Janusz J. Zwiazek.

D. Moret-Fernández (✉) · B. Latorre
Estación Experimental de Aula Dei, Consejo Superior de Investigaciones Científicas (EEAD-CSIC), POB 13034, 50080 Zaragoza, Spain
e-mail: david@eead.csic.es

J. Tormo
Departamento de Ciencias Agrarias y del Medio Natural, Escuela Politécnica Superior, Instituto de Investigación en Ciencias Ambientales (IUCA), Universidad de Zaragoza, Ctra. de Cuarte, s/n 22071, Huesca, Spain

Introduction

Seed germination is defined as the fundamental process by which different plant species grow from a single seed into a seedling. Germination begins with water uptake by the seed (imbibition) and ends with the emergence of the embryonic axis (usually the radicle) through the structures surrounding it (Bewley et al. 2013). Seed imbibition, which marks the period

when a seed changes from an anhydrous to a fully hydrated organism (Vertucci 1989), is a crucial phase for seed germination, without which no germination is possible. This process is required for the resumption of metabolism and initiation of cellular events leading to radicle emergence.

Seed imbibition is controlled by three factors: the initial moisture content of the soil, the temperature of the medium, and the rate at which water is taken up (Pollock 1969). While the first two components are controlled by the environment, the last factor is a function of both the environment and the intrinsic properties of the seed. During seed imbibition, there is an influx of water into the seed promoted by a difference in water potential (h) between the seed and the surrounding medium (Bewley et al. 2013). Continued availability of water to the seed will depend on the relationship between seed and soil water potentials. During the initial steps of the seed imbibition, there is a rapid increase of seed weight due to a high seed-soil water potential gradient. However, as water is absorbed into the seed, h of the seed becomes less negative as the cellular components become hydrated and the water potential gradient for water uptake decreases. This slows the rate of water uptake, which approaches a plateau or slow increase in water content (Bewley et al. 2013). The duration of imbibition depends on certain inherent properties of the seed and on the prevailing conditions during hydration, and imbibition rates can vary according to the different parts of a seed (Vertucci 1989). Further water uptake is dependent primarily upon embryo growth associated with completion of germination and subsequent seedling growth (Bewley et al. 2013). Regarding to the effect of temperature on imbibition process, while Wol et al. (1989) observed that temperature had a little influence on seed imbibition, Abu-Ghannam and McKenna (1997), Khazaei and Mohammadi (2009) and Shafaei, and Masoumi (2014) found that its effect could be considered negligible.

The cumulative imbibition curve of seeds as function of the external water potential can be measured in laboratory using Polietilenglicol (PEG) solutions (Lawlor 1970; Michel 1983), which generates a potential that is assumed to be equal to the soil matric potential (Sharma 1973; Steuter et al. 1981). Increasing concentrations of PEG results in more negative water potentials. Given that water uptake depends on the relationship between the water potential of

the seed and that of the germination medium (Bewley et al. 2013), the imbibition rate of a dry seed will decrease with the increase of the PEG concentrations. Thus, an increasing range of water potentials reduce imbibition in seeds and allow the determination of germination thresholds (Bewley et al. 2013). PEG solutions have been widely used in germination experiments, such as experiments to determine hydrothermal thresholds (Frischie et al. 2019), seed priming experiments (Santini et al. 2017) or to study seed imbibition (Vertucci 1989). However, despite the great efforts made to study the kinetics of seed imbibition (Vertucci 1989; Shafaei and Masoumi 2014) or the relation between imbibition and h (Hadas 1976), to date there are very few works that have analyzed the interaction between seed imbibition and the surrounding medium. For instance, Williams and Shaykewich (1971) showed that the soil hydraulic conductivity could be a limiting factor in the germination process, and Hadas and Russo (1974) observed that the decrease in the soil hydraulic conductivity reduced the rates of water uptake and germination. More recently, Camacho et al. (2021), showed that hydraulic conductivity, rather than h, is a more informative variable to predict both total seed germination rate in soil. In conclusion, it can be stated that the kinetics of water uptake into seeds is influenced by the properties of the seed, as well as by the environment in which it is imbibing (McDonald et al. 1994; Salanenka and Taylor 2011). In addition, seed permeability is influenced by morphology, structure, composition, initial moisture and temperature of imbibition (Vertucci 1989; Bewley et al. 2013).

To date, several models have been developed to simulate the seed germination process. All of them, which focus on capturing the three phases of the soaking process, are based on empirical formulations that employ polynomial (Pimenta et al. 2014), sigmoidal (Demirhan and Özbek 2015) or logistic models (Peleg 1988; da Silva et al. 2018), among others. However, although the estimated parameters represent information that elucidates the germination process, these models are based on empirical functions fittings that do not consider the hydraulic characteristics of the seeds, essential properties for simulating seed imbibition when immersed in soils with contrasting hydraulic properties.

Despite all these advances, to date there is no physical model to quantify the kinetics of seed imbibition,

nor methods to characterize the properties that regulate the seed imbibition process. If we assume that seed imbibition is a physical process (Hegarty 1978), this process should be able to be described by the laws of hydraulic flow, which involve the hydraulic conductivity, *K*, and the water potential difference between the seed and its surroundings. Consequently, if the boundary conditions of experiments studying water infiltration in soils are similar to those for seed imbibition, the same equations used in soil physics could be employed to describe the seed kinetics (Vertucci 1989). Taking these assumptions into account, seeds could be considered as a kind of porous black box with average hydraulic properties. Based on this hypothesis, the same methods used to characterize the hydraulic properties of soils could be applied to characterize the seed kinetics. This methodology could be, for example, the one developed by Moret-Fernández et al. (2016a), in which soil hydraulic properties of a soil column are determined from the inverse analysis of multiple cumulative capillary absorption curves measured at different tensions. By analogy, the hydraulic properties of a seed could be characterized, for example, from the inverse analysis of a set of cumulative imbibition curves measured for a seed immersed in different PEG solutions, PEG concentrations that infer different water potentials. However, as PEG solutions do not reproduce soil conditions (Camacho et al. 2021), their use should be, in principle, limited to laboratory conditions. Knowing the hydraulic properties of the seeds, it would be then possible to simulate seed imbibition in very different scenarios (e.g. different soil in varied environmental conditions).

The objective of this work is to present a new methodology to determine the hydraulic properties of a seed during the imbibition process, data from which the seed imbibition process could be modeled. The methodology is based on the hypothesis that seed imbibition is a physical process resulting from the interaction between surrounding soil and seed water potentials. Taking this concept into account, the seed is then considered as a homogeneous black box porous material in which the water flow is governed by hydraulic properties characteristic of soils. Consequently, the same models applied in soil hydraulics can be applied to seeds. Using HYDRUS-2D, the hydraulic properties of a seed were estimated from the inverse analysis of several cumulative imbibition curves generated on synthetic seeds submerged in different boundary water potentials. A theoretical analysis was first performed to verify the number of external water potentials necessary to accurately estimate the hydraulic properties of a seed. In a second phase, a laboratory methodology was developed to validate and apply the theoretical analysis to experimental imbibition measures. To this end, 3 different seed species were used.

Material and methods

Hydraulic model

The water retention (Eq. 1) and hydraulic conductivity (Eq. 2) functions used to characterize the hydraulic behavior of a seed corresponded to the van Genuchten (1980) and Mualem (1976) models, which have been widely validated and used worldwide in soil hydrology studies. These functions are expressed as

$$\theta(h) = \theta_r + \left(\theta_s - \theta_r\right)\left[\frac{1}{1 + (\alpha h)^n}\right]^m \tag{1}$$

$$K(h) = K_s \frac{\left\{1 - (\alpha h)^{n-1}\left[1 + (\alpha h)^n\right]^{-m}\right\}^2}{\left[1 + (\alpha h)^n\right]^{\frac{m}{2}}} \tag{2}$$

h is the water pressure head or water potential, [L], θ_s and θ_r are the saturated and residual volumetric water content [$L^3 L^{-3}$], K_s is the saturated hydraulic conductivity [$L\ T^{-1}$], α [L^{-1}] and *n* [−] are a scale and shape parameter, respectively, and *m = 1 − 1/n*. According to van Genuchten (1980), θ_r is defined as the water content for which the gradient *dθ/dh* becomes zero.

Inverse analysis to estimate the seed hydraulic properties

According to Eqs. (1) and (2), the hydraulic characterization of a single seed requires knowing the θ_s, θ_r, K_s, α and *n* parameters. Assuming θ_r and θ_s as known values, α, *n* and K_s parameters are optimized by minimizing an objective function, *Q* (Eq. 3). This *Q* function represents the difference between a curve resulting from consecutively joining several imbibition curves simulated with HYDRUS 2D (W_{Hy})

at different boundary water potentials and the corresponding experimental (W_o) curve (Latorre et al. 2015; Moret-Fernández et al. 2016a, 2021)

$$Q\left(K_s, \alpha, n\right) = \sqrt{\frac{\sum_1^{N_u}\left(W_o\left(t_i\right) - W_{Hy}\left(t_i\right)\right)^2}{N_u - 1}} \qquad (3)$$

where N_u is the number of measured, W values, $W_o(t_i)$ and $W_{Hy}(t_i)$ are specific measurements at time t_i. Minimization of the objective function Q was accomplished by a brute-force search (Pardalos and Romeijn 2002), which enumerates all possible candidates of α, n and K_s to a certain precision and selects the best result.

Numerical experiments

Two different numerical experiments were considered. The first one consisted of optimizing K_s, α and n from the inverse analysis of a multiple-tension imbibition curve generated on a synthetic seed. For this purpose, a synthetic and hypothetical porous material of a size similar to that of a barley seed (Fig. 1) was defined. The theoretical θ_r, θ_s, K_s, α, and n, were empirical values fixed to 0.59 and 0.08 cm^3 cm^{-3}, 5.64 10^{-9} cm h^{-1}, 3.8 10^{-5} cm^{-1} and 1.80, respectively. Since the objective of the numerical experiment is to validate the feasibility of the method, the selected θ_r, θ_s, K_s, α, and n should not necessarily correspond to actual hydraulic properties of seeds.

Correct application of the numerical analysis requires to define the initial water potential of the seed, h_i, which was defined in each of the nodes of the mesh generated within the seed (Fig. 1). Because the inverse analysis is performed in the range of tensions,

and since the cumulative imbibition curve depends on initial volumetric water content, θ_i, the θ_i value must be independent of h_i. Otherwise, an incorrect definition of h_i will affect θ_i and thus the shape of the cumulative imbibition curve. To prevent this problem, we assume that θ_i corresponds to that for an air-dried seed, which value is equal to θ_r, or water content persisting in the porous material after a long period of air-drying (Moret-Fernández et al. 2021). According to van Genuchten (1980), θ_r corresponds to the $|h|$ value above which there is no change in water content with increasing values of h. Thus, h_i was defined as the h at the beginning of the flat section of θ_r, and was calculated as h at which θ is 0.01% higher than θ_r. In this case, no significant changes in θ_i can be found for $|h| > |h_i|$ (Fig. 2). The minimum h_i threshold was limited to -10^{20} cm (-10^{16} MPa).

The imbibition curves needed to apply the inverse analysis were generated with the HYDRUS-2D software (Fig. 1). To this purpose, the shape of the synthetic seeds was first delimited. Although it is well known that the seed volume increases in wet seed, a constant seed volume was considered, the value of which corresponded to that of a saturated seed (Table 1).

To simplify the numerical analysis, the seed volume corresponded to the rotation of a plane defined around the z-axis (Fig. 1). After sizing a saturated seed with a precision caliper, the measured dimensions were plotted in HYDRUS-2D. A contour in the xy plane with the same dimensions and shape than the half of a vertical section of a real seed was defined (Fig. 1). The seed surface was discretized as an unstructured FE-Mesh, where targeted FE mesh was fixed to 0.03 cm. Previous numerical analysis demonstrated that, under this discretization, the solution was grid

Fig. 1 Unstructured FE-Mesh used in HYDRUS-2D to reproduce the longitudinal plane of a (**a**) barley, (**b**) wheat and (**c**) vetch seeds
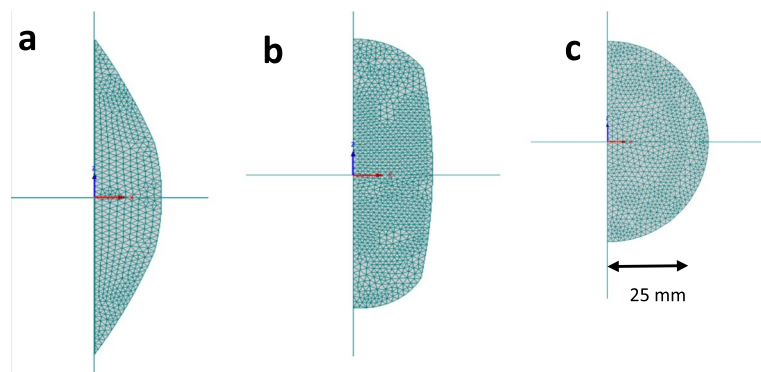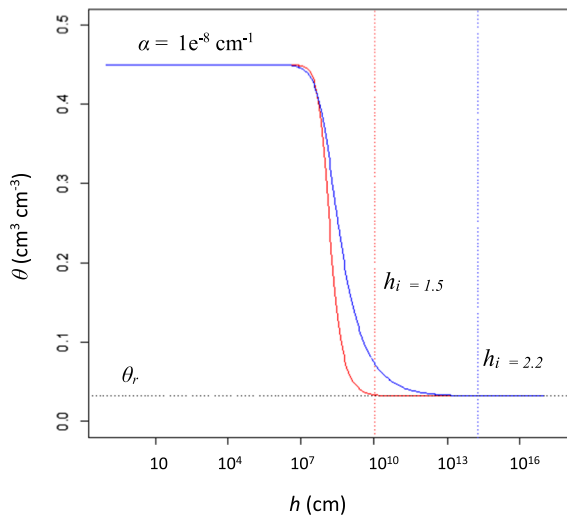
Fig. 2 Example of water retention curves (Eq. 1) with the same α, saturated (θ_s) and residual(θ_r) volumetric water content values, but different values of n (1.5, red line, and 2.2, blue line). h_i denotes the tension, h, at which the volumetric water content, θ, of the respective water retention functions is 0.01% higher than θ_r

independent. Although initial water uptake in seed can occur in specific locations or through inherent structural features in the surrounding tissues (Bewley et al. 2013), a homogeneous seed volume was considered. The time analysis run from 0 to 192 h, and h_i was set to the h value at which θ is 0.01% higher than θ_r.

Once the seed shape and parameters were defined, we proceeded to evaluate the sensitivity of the procedure to estimate K_s, α, and n from the inverse analysis of successive imbibition curves. Given the limited number of parameters, a global sensitivity analysis was used. In this approach, we performed exhaustive evaluations of the model by varying pairs of

variables to discern the input parameters that could be classified as negligible, co-linear, or involved in interactions with other factors. While more efficient sampling methods have been introduced, such as those by Campolongo et al. (2007), our exhaustive approach offers a comprehensive view of the parameter space. This proves especially valuable in inverse analyses where the choice of an optimization method hinges on the characteristics of the error map, including the presence of local minima or elongated valleys. Similar approaches have been used by Simunek and van Genuchten (1996), Simunek and van Genuchten (1997), Simunek et al. (1998) or Peña-Sancho et al. (2017), among others. Thus, four independent synthetic imbibition curves were generated at boundary conditions of 0, -0.5, -1.5 or -2.5 MPa, which values were defined in the external wall of the seed (Fig. 1). These curves were then joined in a series, creating a single curve. Four different scenarios or combinations of imbibition curves with increasing sequences of boundary conditions were evaluated: H_1: 0 MPa; H_2: H_1 + -0.5 MPa; H3: H_2 + -1.5; and H_4: H_3 + -2.5 MPa. The three hydraulic parameters to be optimized, α, K_s and n varied over the ranges $[10^{-8}, 10^{-3}]$ cm^{-1}, $[10^{-13}, 10^{-5}]$ cm h^{-1} and $[1.2, 2.0]$, respectively. The degree of mismatch between theoretical and simulated curves was computed with the Q objective function (Eq. 3), which values were summarized as contours lines or error maps for the three possible combinations: K_s–n, α–n and K_s–α. Within each error maps, the remaining hydraulic parameter was matched to the corresponding theoretical value. The parameter combinations for each response surface were calculated on a rectangular grid, where each parameter was discretized into 40 points, resulting in 1600 grid points by response surface.

Table 1 Weight of a dry at 105 ºC, W_{105_ex}, air-dried, W_{r_ex} and saturated, W_{s_ex}, individual seed, volume of an single air-dried, V_{r_ex} and saturated, V_{s_ex}, seed, bulk density of an air-dried, ρ_{b_r}, and saturated, ρ_{b_s}, individual seed, and saturated, θ_{s_ex}, and residual, θ_{r_ex}, volumetric water content of a single seed averaged from a number of N seeds of barley, wheat and vetch species

	N	$\frac{W_{105\_ex}}{N}$	$\frac{W_{r\_ex}}{N}$	$\frac{W_{s\_ex}}{N}$	$\frac{V_{r\_ex}}{N}$	$\frac{V_{s\_ex}}{N}$	ρ_{b_r}	ρ_{b_s}	θ_{r_ex}	θ_{s_ex}
		g			cm^3		g cm^3		cm^3 cm^{-3}	
Barley	20	0.045	0.048	0.078	0.043	0.058	1.12	0.77	0.08	0.59
Wheat	20	0.045	0.045	0.076	0.044	0.090	0.92	0.45	0.09	0.39
Vetch	10	0.050	0.051	0.098	0.026	0.062	1.76	0.74	0.19	0.85

A second numerical experiment consisting of generating medium- (192 h) and long-time (500 h) seed imbibition curves for boundary tensions of 0, -0.001, -0.01, -0.1, -0.5, -1.5 and -2.5 MPa was performed. These curves were subsequently used to compare the seed water content, θ_f, at the end of the medium- and long-time imbibition experiments, where θ_f was calculated as

$$\theta_f = \left(\frac{W_f - W_d}{W_d}\right)\rho_b \qquad (4)$$

where W_f is the seed water uptake at the end of the corresponding imbibition experiments, and W_d and ρ_b are the dry weight and bulk density of the theoretical seed, which values were fixed to 0.0405 g and 0.768 g cm^{-3}.

Experimental imbibition curves

Three agronomic species were selected: barley (*Hordeum vulgare L.*), wheat (*Triticum aestivum* L) and vetch (*Vicia sativa* L). These were chosen because availability, relatively big size to facilitate manipulation and because, being agricultural varieties, the germination process will be very homogeneous among seeds of the same species. A different number, N, of air-dried seeds, depending of the seed size (Table 1), were used.

The imbibition curves of the experimental seeds correspond to the seed weight increase, $W_{\_ex}$, as a function of time. A total of seven imbibition curves measured in germination tests at water potential of 0, -0.001, -0.01, -0.1, -0.5, -1.5 and -2.5 MPa were recorded. The water potential was simulated using polyethylene glycol (PEG 6000, Polyethylene glycol 6,000, Sigma-Aldrich; MDL Number: MFCD01779614). The appropriate concentration for each level of water potential was determined based on Michel and Kaufmann (1973) equations. Distilled water was used as control. Germination experiments of each species were replicated once.

A set of N air-dried seeds (Table 1) were first weighted to obtain the average initial/residual weight of a seed, W_{r_ex}. These seeds were next placed in a 9-cm diameter Petri dish on a filter paper moistened initially with 8 to 12 ml (depending on the seed size) of either distilled water or PEG solutions. Petri dishes were placed in a dark chamber at 18 ℃ and saturated atmospheric conditions. All seeds were weighted three and two times per day, for the first and remaining days, respectively. To this end, the seeds were extracted from the Petri dishes, excess water was soaked with a dry filter paper, weighted and placed back into the Petri dishes, which were finally returned to the chamber. At the end of each day, the Petri dishes plus the wet seeds were weighted and the loss of water due to seed manipulation was replaced with distilled water or the corresponding PEG solution. Water loss by evaporation was considered negligible due to the short duration of the experiments and the fact the Petri dishes were at saturated atmospheric conditions. The experiment lasted during 5–7 days until constant weight of seed or the emergence of the radicle (or other embryonic tissue) (Bewley et al. 2013) on 80% of seeds placed in the distilled water. In summary, this experiment allowed obtaining an averaged set of cumulative seed imbibition curves (one for each water potential). In this case, 1 g of increase in seed weight corresponds to a 1 cm^3 of water inflow into the seed.

An additional experiment was performed to measure the average initial/residual volumetric water content of a seed, θ_{r_ex}, value that is required by HYDRUS-2D.

$$\theta_{r\_ex} = \left(\frac{W_{r\_ex} - W_{105\_ex}}{W_{105\_ex}}\right)\rho_{b\_r} \qquad (5)$$

where W_{105_ex} is the weight of a set of N seeds after drying them at 105 ℃ during 24 h and ρ_{b_r} is the average bulk density of the air-dry seeds. ρ_{b_r} was calculated according to

$$\rho_{b\_r} = \frac{W_{105\_ex}}{V_{r\_ex}} \qquad (6)$$

where V_{r_ex} is the volume of a set of N seeds, measured as the increase in water height after immersing air-dried seeds in a graduated cylinder with water. To avoid water absorption during V_{r_ex} measurements, the seeds were waterproofed with a silicone spray coating. Since different sets of seeds may have different average volumes and weights and, consequently different values of W_{105_ex} and W_{r_ex}, we will assume that θ_{r_ex} is a constant value within each seed specie.

Since the seed volume changes with seed water content (Bewley et al. 2013), the bulk density of the saturated seed, ρ_{b_s}, was calculated as

$$\rho_{b\_s} = \frac{W_{105\_ex}}{V_{s\_ex}} \qquad (7)$$

where V_{s_ex} is the volume of a set of N seeds measured at saturated seed conditions. To measure V_{s_ex}, a set of N air-dry seeds were placed in a Petri dish with saturated filter paper, until the onset of germination. Next, the hydrated seeds were immersed in the graduated cylinder with water to determine the average value of V_{s_ex}.

Since the sets of seeds used in the imbibition experiments with different PEG solutions have different mean sizes and weights, and consequently can potentially have imbibition curves with different shapes, the optimization process requires sizing and subsequent scaling of the imbibition curves. This process allows that all curves showed the same water absorption at the end of the different imbibition experiments. Within each PEG solution experiment, the dimensioned seed weight, $W_{[0,1]}$, was calculated according to

$$W_{[0,1]} = \frac{W_{ex} - W_{ex\_r}}{W_{ex\_s} - W_{ex\_r}} \qquad (8)$$

where W_{ex_s} is the final weight of the N seed within each PEG experiment, just before seed germination or after flattening of the imbibition curve.

The seed weight, W_o, used in the optimization process was then scaled as

$$W_o = \begin{cases} W_{[0,1]} \dfrac{\overline{W_S}}{\overline{W_{105}}} & if \ W_{[0,1]} < 1 \\[2ex] \dfrac{\overline{W_S}}{\overline{W_{105}}} & if \ W_{[0,1]} \geq 1 \end{cases} \qquad (9)$$

where $\overline{W_S}$ and $\overline{W_{105}}$ are the average weights of seeds at saturation and dried at 105 ºC, respectively. For $\overline{W_S}$ calculation, only curves where seeds were completely saturated were selected. $\overline{W_{105}}$ was calculated as the average value of the dry seeds measured in all imbibition experiments, W_{105}, which was calculated according to

$$W_{105} = \frac{\dfrac{W_{r\_ex}}{N}}{\dfrac{\theta_r}{\rho_{b\_r}} + 1} \qquad (10)$$

Finally, the saturated seed value, θ_{s_ex}, required by HYDRUS-2D, was calculated according to

$$\theta_{s\_ex} = \frac{\overline{W_s}}{W_{105}} \rho_{b\_s} \qquad (11)$$

Optimization of experimental imbibition curves

Given that HYDRUS-2D considers only the seed as a porous material, the synthetic seed only can absorb water until the water potential inside the seed equals that outside, at which point the imbibition rate becomes zero. However, since water uptake in real seeds can continue after completion of the imbibition process, i.e., at the time of germination (Bewley et al. 2013), the experimental curves were modified by imposing, at the time of germination (if exists), a flat section equal to seed weight at germination time. This correction indicates that, at the end of the imbibition phase, the seed weight will remain constant. The inclusion of this appendix is based on previous analysis performed on soil upward infiltration experiments Moret-Fernández et al. 2021), which demonstrated that this flat section is essential to estimate the n parameter of the van Genuchten (1980) model (Eq. 1).

The optimization analysis applied to experimental seeds assumes that θ_r and θ_s are known parameters, which experimental values (θ_{r_ex} and θ_{s_ex}) are obtained experimentally from laboratory measurements (Eqs. 5 and 11, respectively). The sizes of the seeds were measured and the corresponding perimeter was plotted in HYDRUS-2D (see Sect. 2.3). However, since the seed volume plotted in HYDRUS-2D should correspond to an average volume of the N seeds measured in laboratory, to ensure that the total volume of the synthetic seed was correctly plotted, preliminary simulations were conducted to ensure that total water absorbed by the synthetic seed matched the corresponding experimental values measured at the time of germination. To this end, the perimeter of the initially plotted seed was iteratively refined until the difference between the measured and simulated total water absorption of the seed was less than 0.1%. In this case, total water absorption corresponds to the flat section of the imbibition curve at the time of germination. Since the final absorbed water at the time of germination is independent on the parameters of K_s, α, and n, seed shape refinement cannot affect the subsequent optimization of hydraulic parameters.

In order to obtain a better definition of the stabilized section of the imbibition curves, and therefore a more accurate optimization (Moret-Fernández et al. 2021), the flat section imposed at the end of the curve measured in distilled water was extended to 192 h. The corrected cumulative seed imbibition curves measured in the different PEG solutions were then used to estimate the hydraulic parameters of a seed. The imbibition curves measured at 0, -0.5, -1.5 and -2.5 MPa of PEG solutions were selected and merged into a single series. Once defined in HYDRUS-2D the measured θ_{r_ex} (Eq. 5) and θ_{s_ex} (Eq. 11) values (Table 1), the optimization process consisted of looking for the combinations of K_s, α, and n that allows the best fit between measured and simulated imbibition curves. A 3D grid with $20\times20x20$ combinations of K_s, α and n was used, where α, K_s and n varied over the ranges [10^{-8}, 10^{-3}] cm^{-1}, [10^{-15}, 10^{-5}] cm h^{-1} and [1.3, 2.8], respectively. Once this first optimization analysis was completed, a second round was carried out to fine-tune optimization, where the selected interval was [80%, 120%] around the optimized n and the same interval in logarithmic scale for α and K_s. The degree of mismatch between measured and simulated curves was also summarized in the K_s–n, α–n and K_s–α error maps. Within each error map, the remaining hydraulic parameter was matched to the corresponding optimized value.

The volumes of the different seeds plotted in HYDRUS-2D, V_{Hy}, were numerically calculated by running the model with $\theta_r=0$ (Table 1), $\theta_s=1$ and a boundary water potential of 0 MPa. Finally, the α, n and K_s values optimized from 0, -0.5, -1.5 and -2.5 MPa of PEG solutions were validated by comparing the experimental imbibition curves measured on PEG solutions of -0.001, -0.01 and -0.1 MPa to the corresponding curves simulated using the optimized K_s, α, and n and measured θ_{r_ex} and θ_{s_ex} values. All these analyses were repeated for three different seed species: barley (*Hordeum vulgare L.*), wheat (*Triticum aestivum L*) and vetch (*Vicia sativa L*).

Statistical analysis

To establish a comparison between the experimental and optimized imbibition curves used for both the estimation of seed hydraulic properties and their subsequent validation, regressions of the form $W = slope * W_{ex} + intercept$ and corresponding regression coefficient (R^2) were performed. The root mean square error (RMSE) between experimental and optimized curves was calculated according to Eq. (3).

Results

Numerical experiments

The imbibition curves of the synthetic barley seed simulated with HYDRUS-2D showed, in all h-boundary conditions, an increase in water content over time, in which the imbibition rate gradually decreases to a final imbibition rate equal to zero (Fig. 3).

Overall, robust fits were observed between theoretical and optimized curves for scenarios H$_1$ ($R^2=1$; $y=0.99x - 2.2\ 10^{-4}$), H$_2$ ($R^2=1$; $y=0.99x - 1.6\ 10^{-4}$), H$_3$ ($R^2=1$; $y=0.99x - 2.1\ 10^{-4}$) and H$_4$ ($R^2=1$; $y=0.99x - 3.6\ 10^{-4}$) (Fig. 3). However, while similar contours, with a well-defined minimum, were observed in the α-n and K_s-n error maps of scenarios
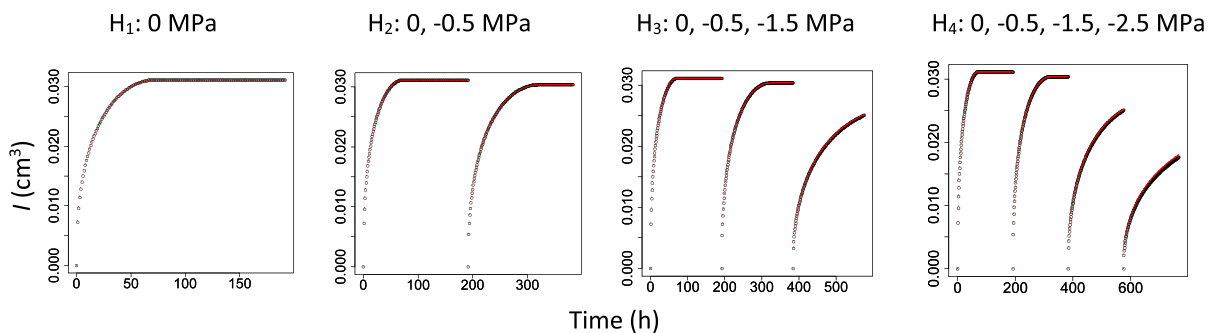
Fig. 3 Theoretical (red circles) and optimized (black circles) cumulative imbibition curves of a synthetic seed obtained for three different combination of boundary seed tensions

H_1, H_2, H_3 and H_4, a completely different behavior was found it the K_s-α plane (Fig. 4). In this last case, while H_1 showed a K_s-α error map with an elongated valley (indicating that infinite combinations of α-K_s can result in nearly identical imbibition curves), the error maps in the remaining scenarios (H_2, H_3 and H_4) tended to a well, the definition of which improved as additional tensions were incorporated. The optimized K_s, α, and n values obtained for H_4 were 5.88 10^{-9} cm h^{-1}, 3.88 10^{-5} cm^{-1} and 1.78, respectively, which represents an error of 0.2, 0.2 and 1.2% with respect to their corresponding theoretical values.

Overall, a close agreement was observed between the water retention curve generated from the optimized α and n and the total seed water content simulated at the end of a 500-h long-time imbibition process (Fig. 5). However, a significant lower total seed water content in -1.5 and -2.5 MPa experiments was observed at the end of the 192 h experiment. These differences indicate that at 192 h the seed was not yet fully wetted.

Experimental measurements

The average weights, volumes, bulk densities and volumetric water contents of an individual seed for the different seed species are shown in Table 1. The total water absorbed by the seed varied according to the different species, in which vetch and wheat, presented the highest and lowest values of W_{s_ex}, respectively (Table 1; Fig. 6). The average weight and volume of the seeds increased at saturation conditions (Table 1). The seed swelling ratio, calculated as the quotient between V_{s_ex} and V_{r_ex} was 1.35, 2.04, and 2.38 for barley, wheat and vetch respectively. The ratio between ρ_{b_r} and ρ_{b_s} varied according to the different species, being larger for the vetch seed.

Experimental imbibition curves of the three seed species measured at different PEG solutions are showed in Fig. 6. In general, a high imbibition rate was observed in all species during the first steps of seed hydration (Fig. 6), a rate that progressively decreased until it stabilized as an almost flat section. Overall, a significant influence of PEG solution on the seed imbibition curve was observed, where the slope of the cumulative imbibition curves decreases with increasing PEG values.

However, a different behavior in cumulative imbibition curves was observed among the three species

(Fig. 6a). Overall, the cumulative imbibition curve measured in the barley seeds immersed in distilled water showed a sharp slope in the first steps of seed hydration, followed by a general flattening. In contrast, a steeper imbibition curve was observed in vetch (Fig. 6c). Intermediate behavior was found in wheat (Fig. 6b). The response of the imbibition curve to the different PEG solution also varied according to the species. Thus, while barley seeds showed relatively small differences in cumulative imbibition curves between 0 and -0.5 MPa of PEG, these differences were more evident in vetch (Fig. 6c). On the other hand, the differences between the cumulative infiltration curves measured in barley at 0 and -2.5 MPa measured were smaller than those observed in wheat and vetch.

Optimization of experimental measurements

Although the theoretical analysis on synthetic seeds shows that H_2 and H_3 scenarios allow a relatively accurate optimization of the hydraulic properties, to obtain more robust and consistent optimizations, all inverse analyses on experimental seeds were done using scenario H_4. For instance, Fig. 7 shows a robust fit between the cumulative imbibition curves measured in barley at 0, -0.5, -1.5 and -2.5 MPa and the corresponding optimized ones.

The error maps obtained for K_s–n, α–n and K_s–α planes showed a unique and well-defined minimum (Fig. 8). The optimized K_s, n and α values obtained for the three seed species are shown in Table 2. A significant fit was also obtained on the barley imbibition curves measured -0.001, -0.01 and -0.1 MPa of water potential, used to validate the method (Fig. 9a and b).

Overall, significant relationships ($p < 0.001$), with low RMSE values and R^2 and slope of the regression line close to one (Table 2), were found between experimental imbibition curves measured at 0, -0.5, -1.5 and -2.5 MPa and the best optimized ones obtained for the three seed species (Table 2). A significant relationship was also found between the imbibition curves measured at -0.001, -0.01 and -0.1 of water potential on wheat ($R^2 = 0.96$; $y = 0.90x + 0.002$; RMSE $= 0.0024$ cm^3) and vetch ($R^2 = 0.90$; $y = 0.82x + 0.011$; RMSE $= 0.0081$ cm) seeds and the corresponding curves simulated using the optimized hydraulic parameters (Table 2). A good agreement was also obtained between the average
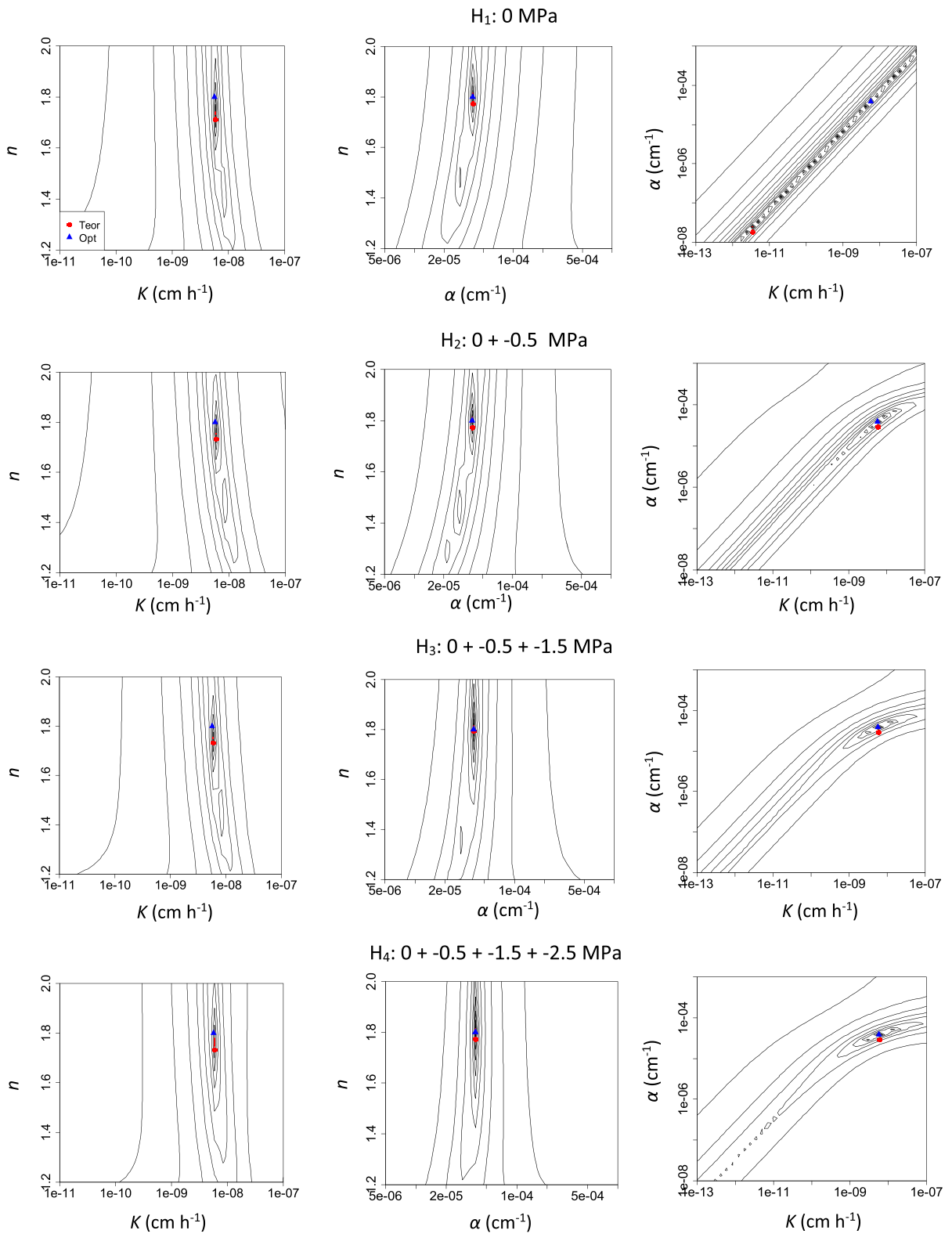
H_1: 0 MPa

H_2: 0 + -0.5 MPa

H_3: 0 + -0.5 + -1.5 MPa

H_4: 0 + -0.5 + -1.5 + -2.5 MPa

volume measured in a single seed (Table 1), $\frac{V_{s\_ex}}{N}$, and the corresponding value numerically calculated with HYDRUS-2D, (Table 2), V_{Hy}, for the different seed species.

The K_s estimated for vetch was one order of magnitude higher than the corresponding values obtained for barley and wheat (Table 2). On the other hand, vetch showed the largest values of α and wheat the highest value of n. The differences in hydraulic parameters observed between seeds (Table 2) resulted in different shapes of water retention and hydraulic conductivity functions (Fig. 10). Compared to wheat and barley, while vetch showed the highest saturated hydraulic conductivity, the corresponding unsaturated values started to decrease at less negative water potentials (i.e. 10^3 cm). Minor differences were observed between barley and wheat seeds.

Discussion

Numerical experiments

The shape of the seed imbibition curves (Fig. 3), which were similar to that observed in soil capillary processes (Moret-Fernández et al. 2016a), indicates that the synthetic seed absorbs water until saturation. Although this curve does not exactly correspond to a complete seed hydration curve during germination, where it can lead to increased water absorption after embryonic axis emergence (Bewley et al. 2013), this shape is representative of the first steps of the seed germination, also referred to as the imbibition phase.

Although all H_1, H_2, H_3 and H_4, scenarios allowed good fit between theoretical and optimized imbibition curves, the sensitivity analysis of the imbibition curves (Fig. 4) indicates that while K_s and α can be satisfactorily optimized from a single imbibition curve at saturation boundary conditions, the n parameter, which defines the slope of the seed water retention curve (Fig. 2), requires additional boundary water potentials. A similar behavior was observed

by Hudson et al. (1996) or Moret-Fernández et al. (2016a) in multi-tension water absorption experiments performed on soils columns or by Simunek and van Genuchten (1997) using multiple tension disc infiltrometer data. On the other hand, although the K_s-α error map in H_2 shows a relatively well-defined well, the well contour improves significantly in the H_3 and H_4 scenarios. These results suggest that accurate estimates of hydraulic properties require the inclusion of very negative water potentials.

Taken θ_r and θ_s as known values, the good agreement between theoretical and optimized K_s, α, and n, indicate that the proposed inverse analysis provides reliable estimations of the seed hydraulic properties when highly negative water potentials are considered.

Finally, comparison between water retention curves generated from the optimized α and n and the total seed water content simulated at the end of a 192 and 500 h long-time imbibition process (Fig. 5) showed that the fit with respect to the optimized retention curve improved when long imbibition times are considered. This behavior is explained by the fact that seed imbibition is governed by an extremely low value of K_s (Table 2), hydraulic conductivity value that slows down the process of water absorption. However, although these results may
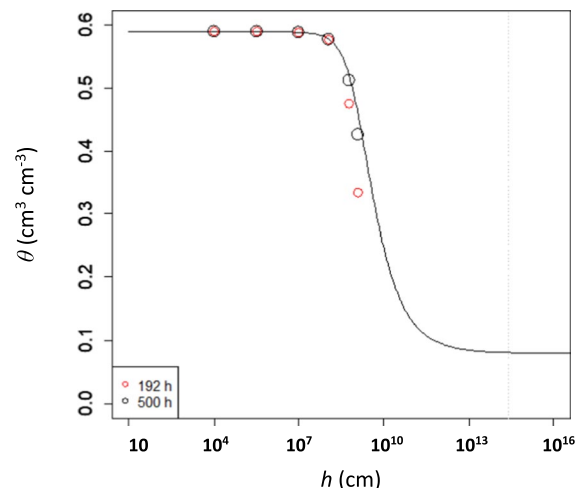
Fig. 5 Water retention curve (continuous line) generated with the optimized α and n values obtained from the inverse analysis of a series of cumulative imbibition curves of a synthetic seed, and the simulated total seed water content at the end of a120 h simulation (red circles) and at time of imbibition curve stabilization (500 h) (black circles)
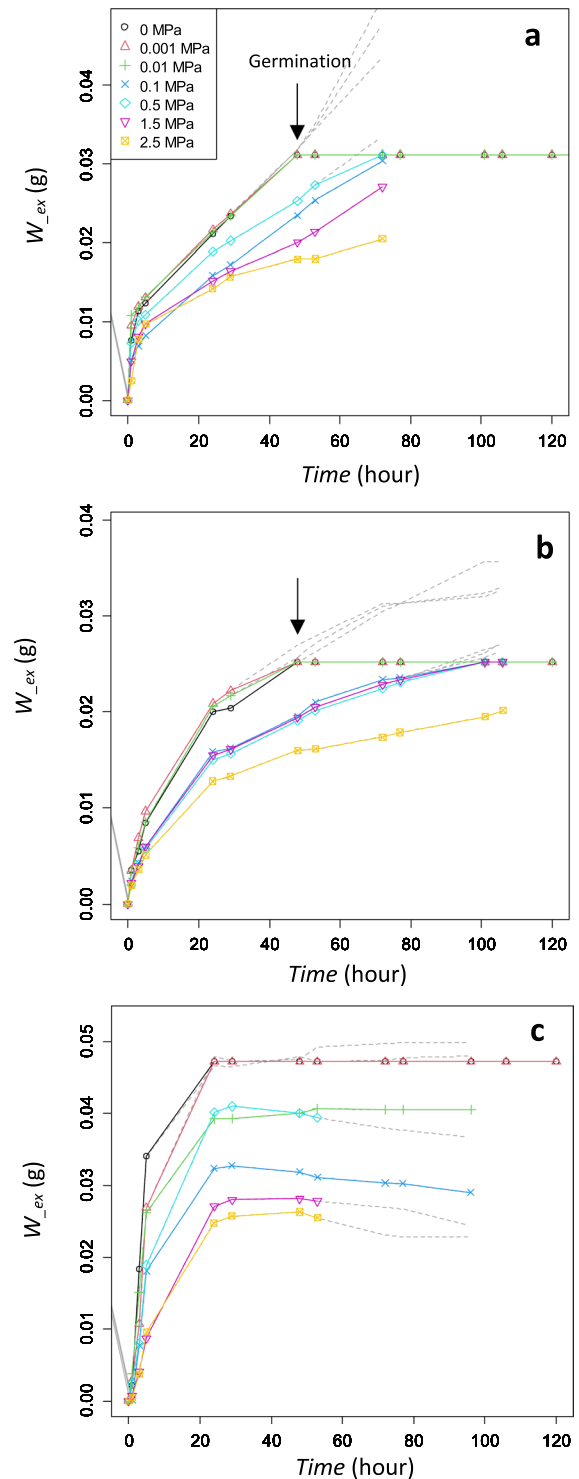
Fig. 6 Cumulative imbibition curves measured in **a** barley, **b** ▶ wheat and **c** bean seeds immersed in different solutions PEG ranging from 0 to -2.5 MPa. The continuous colored lines indicate the imbibition curves that have flattened just after germination, and the dashed greys ones are the continuation of the corresponding measured imbibition curves. Vertical arrows indicate the time of germination. W_{ex} is the average weight of the corresponding set of seeds. No germination was observed in vetch

suggest that the water retention curve can theoretically be estimated from the seed water content once the imbibition curve has been stabilized, we think it is more efficient to estimate the seed hydraulic properties from the inverse analysis of several transient imbibition curves, since it allows (i) to drastically reduce the duration of the experiment and the number of tensions required, (ii) to simultaneously estimate the water retention and hydraulic conductivity functions, and (iii) to eliminate the problems of seed rotting when seeds are left for long periods of time in PEG solutions.

Experimental measurements

In general, the measured θ_{r_ex} and θ_{s_ex} values were close to the range of [5, 15] % and [40, 50] % values, respectively, reported in the literature (Bewley et al. 2013). The high imbibition rate observed in all species during the first steps of seed hydration (Fig. 6) should be attributed to the large difference in water potential between the seed (around -50 to -350 MPa, Bewley et al. 2013) and the surrounding medium. However, as water is absorbed by the seed, the matric potential of the seed becomes less negative, which decreases the gradient and thus the rate of water absorption. At time of germination, seed tension should come into near equilibrium with that of the external water source, which translates to the flat section imposed in the cumulative imbibition curve at time of germination.

The significant decrease of the cumulative imbibition curve with increasing PEG solutions corroborate that the imbibition rate decreases as the gradient between internal and external seed water potential decreases (Vertucci 1989; Bewley et al. 2013). Finally, the different shapes of imbibition curves observed among the three seed species, suggest that there must be a different hydraulic behavior among these seeds (Vertucci 1989).
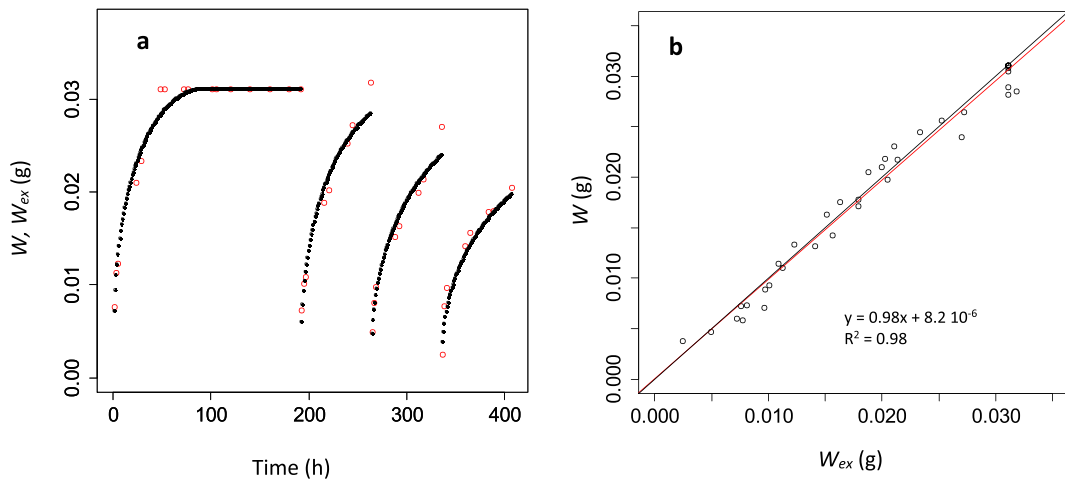
Fig. 7 (**a**) Measured (red circles) and optimized (black circles) cumulative imbibition curves (0, -0.5 and -2.5 MPa) of barley seeds, and (**b**) corresponding linear regression analysis. W_{ex} and W are average measured and simulated weights of a barley seed, respectively
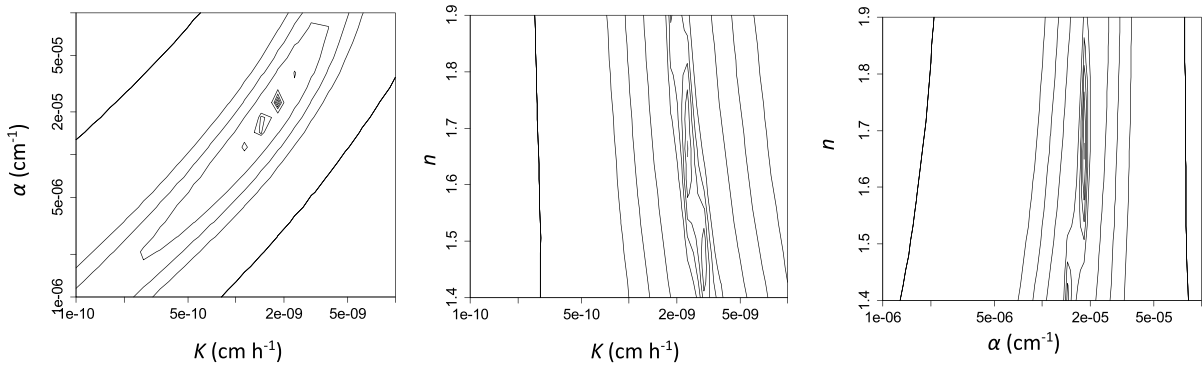

Fig. 8 Response surfaces for K_s-α, α-n and K_s-n planes calculated for a series of cumulative imbibition curves (0, -0.5 and -2.5 MPa) measured from a sample of barley seeds. Red line is the contour line corresponding to 5% of the minimal value of the objective function, Q (Eq. 3)

Table 2 Seed volume numerically calculated with HYDRUS-2D, V_{Hy}, saturated hydraulic conductivity, K_s, and α, n parameters of the water retention curve optimized from the inverse analysis of imbibition curves measured on barley, wheat and bean seeds immersed in PEG solutions of 0, -0.5, -1.5 and -2.5 MPa. RMSE, R^2 and *Regression function* denote the root mean square error, the coefficient of determination and the function resulting of the linear regression between experimental and best optimized imbibition curves measured for the three seed species

	V_{Hy}	K_s	α	n	R^2	*Regression function*	*RMSE*
	cm^3	cm h^{-1}	cm^{-1}				cm^3
Barley	0.061	2.34 10^{-9}	1.83 10^{-5}	1.66	0.98	y = 0.98x + 8.2 10^{-6}	0.0011
Wheat	0.104	9.16 10^{-10}	1.51 10^{-5}	1.89	0.97	y = 0.90x + 0.002	0.0017
Vetch	0.072	6.16 10^{-8}	6.16 10^{-5}	1.62	0.95	y = 0.85x + 0.006	0.0025
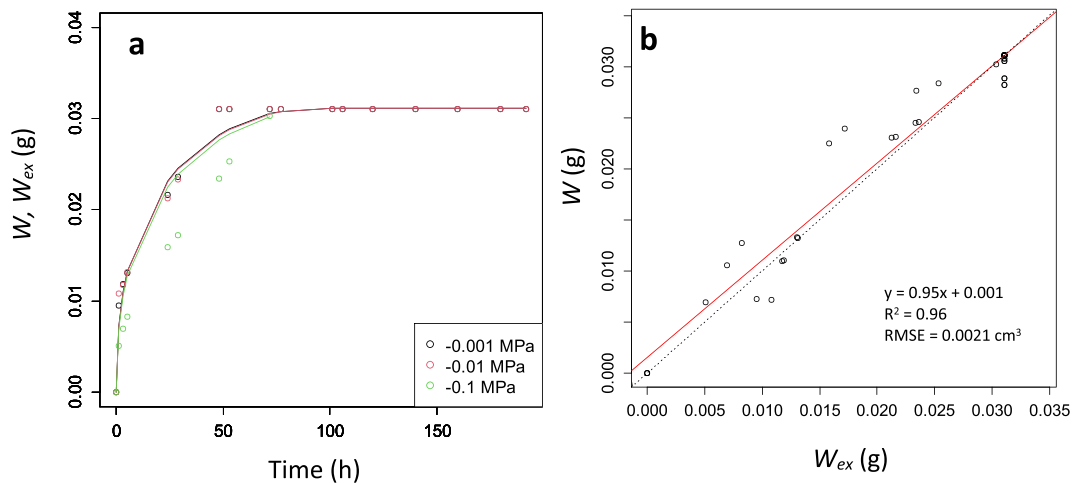
Fig. 9 a) Measured (circles) at -0.001, -0.01 and -0.1 MPa of barley seed boundary tensions and corresponding simulated cumulative imbibition curves obtained from optimized hydrau-

lic parameters (Table 2), and (**b**) corresponding linear regression analysis. W_{ex} and W are average measured and simulated weights of a barley seed, respectively

Optimization of experimental measurements

The robust fit between the imbibition curves measured in barley seeds and the corresponding optimized ones (Fig. 7, Table 2) suggests the model can be also applied to real seeds. The unique and well-defined minimum showed in the K_s–n, α–n and K_s–α error maps of barley seeds (Fig. 8) indicates that there is a unique combination of K_s, n and α that allows a better fit over the curves measured at water potentials at 0, -0.5, -1.5 and -2.5 MPa. Similar results were obtained by Simunek and van Genuchten (1997) and Moret-Fernández et al. (2016a) working in multiple tension experiments applied to soils. The significant fit, with low RMSE value, obtained on the barley imbibition curves measured -0.001, -0.01 and -0.1 MPa of water potential (Fig. 9) validates that the inverse analysis can be applied to experimental seeds, whose optimized values can be assumed to correspond to mean hydraulic properties of a set of seeds. The good agreements also obtained in vetch and wheat seeds (Table 2) confirm the robustness of the method.

The different values of hydraulic properties obtained between the three seeds species (Table2) should be related to the different cumulative imbibition curves measured in the three species. Thus, the higher K_s obtained in vetch, which indicates larger capacity to uptake water at near saturated conditions, is consistent

with the faster imbibition process of this seed in distilled water (Fig. 6c). Furthermore, the larger value of α in vetch, which suggest a faster decrease of $K(h)$ at relatively low negative values of water potentials (Fig. 10), agrees with the significant lower water uptake of this seed at -1.5 and -2.5 MPa (Fig. 6c), and suggests that vetch is more sensitive to high negative water potentials. The opposite behavior of α observed in barley and wheat resulted in faster water imbibition at more negative water potential. These results would suggest that, while vetch is a seed adapted to rapid germination under favorable water conditions, barley and wheat can probably hydrated under more restrictive conditions of water potential.

However, in spite the good fits obtained between experimental and optimized imbibition curves, further efforts should be done to overcome the simplifications assumed in the paper, such as the constant volume of the seed assumed during the imbibition process or the homogeneous distribution of the hydraulic properties within in the seed volume. On the other hand, alternative techniques, such as photogrammetry (Moret-Fernández et al. 2016b) or laser rangefinder (Rossi et al. 2008), should be also considered to obtain a more accurate reproduction of the seed shape. Finally, it should be noted that this work is only intended to show a new procedure to estimate the hydraulic properties of a seed, and do not statistically compare hydraulic properties within
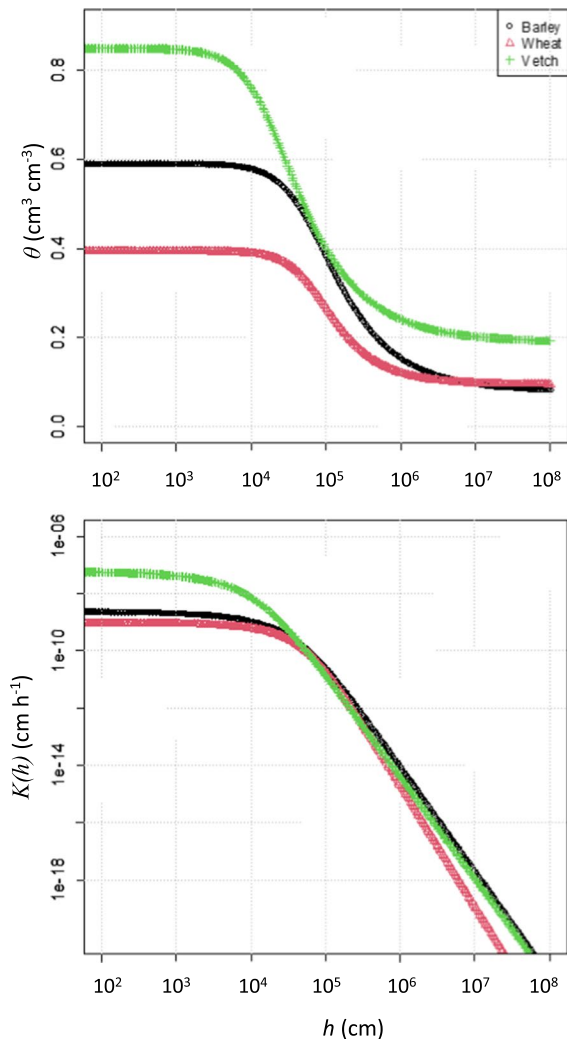
Fig. 10 (**a**) Water retention curves and (**b**) hydraulic conductivity functions calculated for barley, wheat and bean seeds by applying the optimized the θ_s, K_s, α and n parameters (Table 2) to Eq. (2) and (3), respectively

and between different species. For this last point, replications of seed measurements and the corresponding analysis of variance should be included. Currently, PEG experiments applied in seed ecology studies are used to establish the water potential threshold below which seeds cannot germinate (Dürr et al. 2015; Frischie et al. 2019) and it is assumed that germination at very negative water potentials is an indicator of adaptation to arid environments. However, based on results obtained in this work, seed hydraulic properties could be used as a new

indicator to study seed adaptation to aridity. Thus, while K_s would be an indicator of the capacity of a seed to absorb water at near saturation conditions, the α and n parameters would indicate the capacity of seed to imbibe under water stress. This methodology could also be useful to study the changes of seeds from dormant to non-dormant states, changes that depend on the hard, impermeable layers that surround the seeds (Penfield 2017), or to distinguish whether the lack of imbibition is due to the existence of a very negative potential germination threshold or to a very low K_s due to the impermeable seed coat. Finally, the application of this methodology would also allow us to understand the role of the shape and size of the seeds (Wang et al. 2004; Dias Laumann et al. 2023) or the presence of awns, wings, hairs, elaiosomes or mucilage on the imbibition process (Bochenková et al. 2017, De Paula 2015 or López-Vila and García-Fayos 2005).

Conclusions

The seed can be considered as a porous material, which hydraulic properties can be estimated from the inverse analysis of several imbibition curves measured at different boundary water potentials. Therefore, we present a new methodology to determine the hydraulic conductivity function and water retention curve of a seed during the imbibition process and demonstrate its feasibility. This new methodology can be used in very different fields involving seed imbibition (agronomy, forestry, restoration ecology or seed ecology). In addition, these new findings could serve as cornerstone to simulate and study the seed imbibition process in any scenario, that, until now, have been difficult to reproduce. For instance, this new information will allow study and simulate the effect of soil type on the hydration process, the rate of seed hydration as a function of sowing depth, define optimal germination windows as a function of climatic conditions and soil type, or assess the relationship between seed morphology and the hydraulic properties of the adjacent soil, among others.

References

Abu-Ghannam N, McKenna B (1997) Hydration kinetics of red kidney beans (*Phaseolus vulgaris* L.). J Food Sci 62:520–523

Bewley JD, Bradford KJ, Hilhorst HWM., Nonogaki H (2013) Seeds: physiology of development, germination and dormancy, 3rd Edition, https://doi.org/10.1007/978-1-4614-4693-4_4

Bochenková M, Karlík P, Jiras HM, P, (2017) Does seed modification and nitrogen addition affect seed germination of Pulsatilla grandis? Sci Agric Bohem 48:216–223. https://doi.org/10.1515/sab-2017-0029

Camacho ME, Heitman JL, Gannon TW, Amoozegar A, Leon RG (2021) Seed germination responses to soil hydraulic conductivity and polyethylene glycol (PEG) osmotic solutions. Plant Soil 462:175–188. https://doi.org/10.1007/s11104-021-04857-5

Campolongo F, Cariboni J, Saltelli A (2007) An effective screening design for sensitivity analysis of large models. Environ Mod Soft 22:1509–1518

da Silva AR, Leão-AraújoEF RBR, dos Santos WV, Santana HA, Silva SCM, Fernandes NA, Costa DS, Mesquita JCP (2018) Modeling the three phases of the soaking kinetics of seeds. Agron J 110:164–170

Demirhan E, Özbek B (2015) Modeling of the water uptake process for cowpea seeds (*Vigna unguiculata* L.) under common treatment and microwave treatment. J Chem Soc Pak 37:1–10

De Paula OC, Marzinek J, Oliveira DMT, Paiva EAS (2015) Roles of mucilage in Emilia fosbergii, a myxocarpic Asteraceae: Efficient seed imbibition and diaspore adhesion. Am J Bot 102:1413–1421

Dias Laumann P, Cardoso Ferreira M, Alves da Silva D, Mascia Vieira DL (2023) Germination traits explain the success of direct seeding restoration in the seasonal tropics of Brazil. Forest Ecol Manag 529:120706. https://doi.org/10.1016/j.foreco.2022.120706

Dürr C, Dickie JBB, Yang XY, Pritchard HW (2015) Ranges of critical temperature and water potential values for the germination of species worldwide: Contribution to a seed trait database. Agric Forest Meteor 200:222–232. https://doi.org/10.1016/j.agrformet.2014.09.024

Frischie S, Fernández-Pascual E, Ramirez CG, Toorop P, González MH, Jiménez-Alfaro B (2019) Hydrothermal thresholds for seed germination in winter annual forbs from old-field Mediterranean landscapes. Plant Biol 21 https://doi.org/10.1111/plb.12848

Hadas A (1976) Water uptake and germination of leguminous seeds under changing external water potential in osmotic solutions. J Exp Bot 27:480–489

Hadas A, Russo D (1974) Water uptake by seeds as affected by water stress, capillary conductivity, and seed-soil water contact. I Experimental Study Agron J 66:643–647. https://doi.org/10.2134/agronj1974.00021962006600050012x

Hegarty TW (1978) The physiology of seed hydration and dehydration, and the relation between water stress and the control of germination: a review. Plant, Cell Environ 1:101–119

Hudson DB, Wierenga PJ, Hills RG (1996) Unsaturated hydraulic properties from upward flow into soil cores. Soil Sci Soc Am J 60:388–396

Khazaei J, Mohammadi N (2009) Effect of temperature on hydration kinetics of sesame seeds (*Sesamum indicum* L.). J Food Eng 91:542–552

Latorre B, Peña C, Lassabatere L, Angulo-Jaramillo R, Moret-Fernández D (2015) Estimate of soil hydraulic properties from disc infiltrometer three-dimensional infiltration curve. Numerical analysis and field application. J Hydrol 57:1–12

Lawlor DW (1970) Absorption of polyethylene glycols by plants and their effects on plant growth. New Phytol 69:501–513

López-Vila JR, García-Fayos P (2005) Diplochory in Ulex parviflorus Pourr. Acta Oecologica 28:157–162. https://doi.org/10.1016/j.actao.2005.03.008

McDonald MB, Sullivan J, Lauer MJ (1994) Pathways of water uptake in maize seeds. Seed Sci Technol 22:79–90

Michel BE (1983) Evaluation of the water potentials of solutions of polyethylene glycol 8000 both in the absence and presence of other solutes. Plant Physiol 72:66–70

Michel BE, Kaufmann MR (1973) The osmotic potential of polyethylene glycol 6000. Plant Physiol 51:914–916

Moret-Fernández D, Latorre B, Peña-Sancho C, Ghezzehei TA (2016a) A modified multiple tension upward infiltration method to estimate the soil hydraulic properties. Hydrol Proc https://doi.org/10.1002/hyp.10827

Moret-Fernández D, Latorre B, Peña C, González-Cebollada C, López MV (2016b) Applicability of the photogrammetry technique to determine the volume and the bulk density of small soil aggregates. Soil Res. https://doi.org/10.1071/SR15163

Moret-Fernández D, Latorre B, López MV, Pueyo Y, Tormo J, Nicolau JM (2021) Hydraulic properties characterization of undisturbed cores under different soil managements. CATENA. https://doi.org/10.1016/j.catena.2020.104816

Mualem Y (1976) A new model for predictingthe hydraulic conductivity of unsaturated porous media. Water Resour Res 12:513–522

Pardalos PM, Romeijn HE (2002) Handbook of global optimization, vol. 2. Springer Science & Business Media https://doi.org/10.1007/978-1-4757-5362-2

Penfield S (2017) Seed dormancy and germination. Curr Biol 27:R874–R878. https://doi.org/10.1016/j.cub.2017.05.050

Peña-Sancho C, Ghezzehei TA, Latorre B, Moret-Fernández D (2017) Water absorption-evaporation method to estimate the soil hydraulic properties. Hydrol Sci J 62:1683–1693

Pimenta AC, Zuffellato-Ribas KC, Laviola BG, Panobianco M (2014) Water uptake curve in physic nut seeds. Comun Sci 5:295–301

Peleg M (1988) An empirical-model for the description of the moisture sorption curves. J Food Sci 53:1216–1217. https://doi.org/10.1111/j.1365-2621.1988.tb13565.x

Pollock BM (1969) Imbibition temperature sensitivity of lima beans controlled by initial seed moisture. Plant Physiol 44:907–911

Rossi AM, Hirmas DR, Graham RC, Sternberg PD (2008) Bulk density determination by automated three-dimensional laser scanning. Soil Sci Soc Am J 72:1591–1593. https://doi.org/10.2136/sssaj2008.0072N

Salanenka YA, Taylor AG (2011) Permeability of seed coats of various species. Hort Sci 46:622–626

Santini BA, Rojas-Aréchiga M, García Morales E (2017) Priming effect on seed germination: Is it always positive for cacti species? J Arid Environ 147:155–158. https://doi.org/10.1016/j.jaridenv.2017.07.013

Simunek J, van Genuchten MT (1996) Estimating unsaturated soil hydraulic properties from tension disc infiltrometer data by numerical inversion. Water Resour Res 32:2683–2696

Simunek J, van Genuchten MTh (1997) Estimating unsaturated soil hydraulic properties from multiple tension disc infiltrometer data. Soil Sci 162:383–398

Simunek J, Wendroth O, van Genuchten MT (1998) Parameter estimation analysis of the evaporation method for determining soil hydraulic properties. Soil Sci Soc Am J 62:894–905

Sharma ML (1973) Simulation of drought and its effect on germination of five pasture species. Agron J 65:982–987. https://doi.org/10.2134/agronj1973.00021962006500060041x

Shafaei SM, Masoumi AA (2014) Studying and modeling of hydration kinetics in chickpea seeds (*Cicer arietinum* L.). Agric Communic 2:15–21

Steuter AA, Mozafar A, Goodin JR (1981) Water potential of aqueous polyethylene glycol. Plant Physiol 67:64–67

van Genuchten MT (1980) A closed form equation for predicting the hydraulic conductivity of unsaturated soils. Soil Sci Soc Am J 44:892–898

Vertucci CW (1989) The kinetics of seed imbibition: controlling factors and relevance to seedling vigor. In: Stanwood PC, McDonald MB (eds) Seed Moisture, vol 14. CSSA Special Publications

Wang R, Bai Y, Tanino K (2004) Effect of seed size and subzero imbibition-temperature on the thermal time model of winterfat (*Eurotia lanata,* Pursh) Moq.). Environ Exp Botany 51:183–197. https://doi.org/10.1016/j.envexpbot.2003.10.001

Williams J, Shaykewich CF (1971) Influence of soil water matric potential and hydraulic conductivity on the germination of rape (*Brassica napus* L.). J Exp Botany 22:586–597. https://doi.org/10.1093/jxb/22.3.586

Wol W, Dillonm D, Copeland PF, Dilley LF (1989) Imbibitional damage and temperature. Plant Physiol 89:805–810